KU LEUVEN

STADIUS
Center for Dynamical Systems, Signal Processing and Data Analytics

Citation/Reference	Verdyck J., Moonen M. (2017), **Dynamic Spectrum Management in Digital Subscriber Line Networks with Unequal Error Protection Requirements** IEEE Access, vol. 5, no. 1, Dec. 2017, pp. 18107 - 18120.
Archived version	Published manuscript
Published version	http://dx.doi.org/10.1109/ACCESS.2017.2748359
Journal homepage	http://ieeexplore.ieee.org/xpl/RecentIssue.jsp?punumber=6287639
Author contact	jeroen.verdyck@esat.kuleuven.be *+ 32 (0)16 324723*
Abstract	Digital subscriber line (DSL) technology remains the most popular broadband access technology. A variety of algorithms has been developed to improve performance in DSL networks, which are commonly referred to as dynamic spectrum management (DSM) algorithms. The main goal of these algorithms is to fight crosstalk between different lines in a cable bundle. Current DSM algorithms provide an equal level of error protection for each serviced application and each user. However, different applications may have unequal error protection (UEP) requirements. The equal level of error protection usually provided by DSM algorithms may then be excessive for some applications, which leads to a waste of valuable resources. This paper, therefore, considers DSM for DSL networks providing UEP. Four joint signal and spectrum coordination algorithms are presented, enabling a different level of error protection for different applications. These algorithms are modified versions of existing optimal spectrum balancing and distributed spectrum balancing algorithms for joint signal and spectrum coordination in upstream as well as downstream DSL. In addition, an algorithm is presented which, for each application, selects a suitable modulation and coding (MC) scheme from a set of admissible MC schemes. Through simulations, it is shown that DSM with UEP can indeed lead to moderate performance gains.
IR	https://lirias.kuleuven.be/handle/123456789/597376

(article begins on next page)

IEEE Access
Multidisciplinary | Rapid Review | Open Access Journal

Received August 9, 2017, accepted August 28, 2017, date of publication September 1, 2017, date of current version September 27, 2017.

Digital Object Identifier 10.1109/ACCESS.2017.2748359

Dynamic Spectrum Management in Digital Subscriber Line Networks With Unequal Error Protection Requirements

JEROEN VERDYCK, (Student Member, IEEE), AND MARC MOONEN, (Fellow, IEEE)
ESAT/STADIUS, Stadius Center for Dynamical Systems, Signal Processing and Data Analytics, KU Leuven, 3001 Leuven, Belgium

Corresponding author: Jeroen Verdyck (jeroen.verdyck@esat.kuleuven.be)

This research work was carried out at the ESAT Laboratory of KU Leuven, in the frame of the Interuniversity Attractive Poles Programme initiated by the Belgian Science Policy Office: IUAP P7/23 Belgian network on stochastic modeling analysis design and optimization of communication systems (BESTCOM) 2012–2017, Research Project FWO under Grant 0912.13 Cross-layer optimization with real-time adaptive dynamic spectrum management for fourth generation broadband access networks, VLAIO O&O Project under Grant HBC.2016.0055 5GBB Fifth generation broadband access. The scientific responsibility is assumed by its authors.

ABSTRACT Digital subscriber line (DSL) technology remains the most popular broadband access technology. A variety of algorithms has been developed to improve performance in DSL networks, which are commonly referred to as dynamic spectrum management (DSM) algorithms. The main goal of these algorithms is to fight crosstalk between different lines in a cable bundle. Current DSM algorithms provide an equal level of error protection for each serviced application and each user. However, different applications may have unequal error protection (UEP) requirements. The equal level of error protection usually provided by DSM algorithms may then be excessive for some applications, which leads to a waste of valuable resources. This paper, therefore, considers DSM for DSL networks providing UEP. Four joint signal and spectrum coordination algorithms are presented, enabling a different level of error protection for different applications. These algorithms are modified versions of existing optimal spectrum balancing and distributed spectrum balancing algorithms for joint signal and spectrum coordination in upstream as well as downstream DSL. In addition, an algorithm is presented which, for each application, selects a suitable modulation and coding (MC) scheme from a set of admissible MC schemes. Through simulations, it is shown that DSM with UEP can indeed lead to moderate performance gains.

INDEX TERMS DSL, crosstalk, optimization, dynamic spectrum management, unequal error protection, multiple access channel, broadcast channel.

I. INTRODUCTION

From the vantage point of other layers in the OSI model, the digital subscriber line (DSL) physical layer can be modeled as a single connection per user, through which it can send data at a certain data rate and with a particular level of error protection. The DSL physical layer uses discrete multitone (DMT) modulation, and hence effectively consists of many parallel connections, corresponding to the individual tones. Usually, the same bit error rate (BER) is achieved across tones, as otherwise the BER of the entire system would be dominated by the tone with the highest error rate. However, when a collection of different applications is serviced, there will be differences in the level of error protection that is appropriate for each application. Such differences can even exist within one application, e.g. when a source encoder yields data with different levels of importance. Unequal error protection (UEP) takes advantage of these differences by dividing the one connection per user into a set of subconnections, each with its own data rate, BER, collection of tones, and channel coding. By accommodating for UEP, further performance gains can indeed be achieved.

In general, the BER is governed by two mechanisms. First, modulation based error control consists of choosing the amount of signal power allocated for different constellations. Second, forward error correction (FEC) based error control consists of selecting a certain channel coding scheme. Current DSL networks implement FEC through Reed-Solomon (RS) error correcting codes and trellis coded

2169-3536 © 2017 IEEE. Translations and content mining are permitted for academic research only.
Personal use is also permitted, but republication/redistribution requires IEEE permission.
See http://www.ieee.org/publications_standards/publications/rights/index.html for more information.

modulation (TCM) [1], [2]. A particular combination of modulation based and FEC based error control will be referred to as a modulation and coding (MC) scheme. Note that different MC schemes can often achieve the same BER. However, these MC schemes do not necessarily result in equal delay or throughput performance. Therefore, care should be taken in choosing an appropriate MC scheme to achieve a specific target BER.

Analogous to error control mechanisms, UEP techniques are classified into two major categories [3]. Transceiver or modulation based UEP schemes constitute the first category, and consist of allocating an unequal amount of transmit power to the constellations of different subconnections. Most modulation based UEP schemes implement either hierarchical modulation [4] or UEP bitloading [4]–[8], the latter of which will be considered in this paper. The second category consists of FEC based UEP schemes, where FEC codes with different rates are used for different subconnections.

Apart from UEP, a variety of algorithms has been developed to improve performance in DSL networks, commonly referred to as dynamic spectrum management (DSM) algorithms [9]. The main goal of these algorithms is to fight crosstalk between different lines in a cable bundle. DSM mainly addresses the problem of interference between different lines in a cable bundle, called crosstalk in the DSL context, which is *the* major source of DSL performance degradation. Increasing demand for higher data rates forces telcos to operate at higher frequencies, at which the crosstalk problem is even more severe.

Three DSM levels are distinguished [10]. Level 1 DSM manages each line individually, at most introducing some politeness in order to mitigate the effects of crosstalk. Higher DSM levels assume some cooperation between lines. In level 2 DSM, the transmit powers of different lines are managed jointly, in order to cooperatively mitigate the effects of crosstalk [11]–[16]. This technique is also referred to as spectrum coordination. Finally, level 3 DSM consists of coordinating multiple lines on the signal level [17]–[19], and is commonly referred to as signal coordination or vectoring. Signal coordination requires the modems of different lines to be co-located, thus introducing a difference between upstream (US) and downstream (DS) transmission. In US transmission, signal coordination is possible at the receiver side only, such that the US system corresponds to a multiple access channel (MAC). Conversely, DS transmission allows signal coordination only at the transmitter, such that the DS system corresponds to a broadcast channel (BC). Combinations of different DSM levels are also possible, and exceedingly high data rates can be achieved by combining signal and spectrum coordination [20]–[24].

Current DSM algorithms consider DSL networks with a single connection per user, and are incompatible with UEP. This paper shows how these DSM algorithms can be adapted in order to support UEP. While previous work focused on UEP adaptations of spectrum coordination algorithms [8], this paper extends the joint signal and spectrum coordination algorithms from [20]–[23] to support UEP. Moreover, the problem of joint DSM and per subconnection MC scheme selection, commonly referred to as adaptive modulation and coding (AMC), is tackled. This paper develops a heuristic algorithm that selects an MC scheme for each subconnection from a set of candidate MC schemes. Furthermore, an upper bound is established which, in simulations, is used to demonstrate that the proposed heuristic algorithm performs very well.

The paper is organized as follows. In Section II, the system model for the MAC and BC is presented, and a description of how UEP is achieved is given. The general problem statement is provided in Section III. Four algorithms for joint signal and spectrum coordination with UEP are derived in Sections IV and V. These algorithms are adaptations of existing optimal spectrum balancing (OSB) and distributed spectrum balancing (DSB) algorithms for joint signal and spectrum coordination in US and DS DSL. AMC is considered in Section VI, where a heuristic algorithm is developed selecting an MC scheme for each subconnection. The performance of the five proposed algorithms is assessed in Section VII.

II. SYSTEM MODEL

The DSL physical layer uses DMT to split the available spectrum into a set of orthogonal carriers or tones that experience flat fading. Assuming no inter-carrier interference occurs, transmission can be modeled for each tone independently. For each tone, the channel is modeled as a multiple access channel (MAC) or a broadcast channel (BC), depending on whether US or DS transmission is considered, where signals are jointly coordinated at the receiver or transmitter side. In case coordination is possible neither at the transmitter nor at the receiver side, such as in CO/RT deployments, the channel is modeled as an interference channel for which UEP spectrum coordination algorithms have been developed in [8].

A. MULTIPLE ACCESS CHANNEL

US transmission in an N-user DSL network can be modeled for each tone independently as

$$\boldsymbol{y}_k = \boldsymbol{H}_k \boldsymbol{x}_k + \boldsymbol{z}_k, \quad \forall k \in \mathcal{K}, \tag{1}$$

where $\mathcal{K}$ denotes the set of K tones. The vector $\boldsymbol{x}_k = \left[x_k^1, x_k^2, \ldots, x_k^N\right]'$ contains the data symbol of all users on tone k, with $(\cdot)'$ denoting the transpose operator. $[\boldsymbol{H}_k]_{n,m} = h_k^{n,m}$ is the $N \times N$ channel matrix containing the transfer function between the transmitter of user m and receiver of user n, evaluated on tone k. Moreover, $\boldsymbol{z}_k$ is a vector of additive Gaussian noise, and $\boldsymbol{y}_k$ contains the received signal for all users on tone k. Also, define $\mathcal{N}$ as the set of N users.

The transmitted symbol power and received noise power of user n on tone k are respectively denoted as $s_k^n = \Delta_f \mathcal{E}\{|x_k^n|^2\}$ and $\sigma_k^n = \Delta_f \mathcal{E}\{|z_k^n|^2\}$, where Δ_f is the tone spacing and $\mathcal{E}\{\cdot\}$ is the expected value operator. Also define

$\boldsymbol{s}_k = [s_k^1, s_k^2, \ldots, s_k^N]'$ as the symbol power vector of tone k. Likewise, define $\boldsymbol{s}^n = [s_1^n, s_2^n, \ldots, s_K^n]'$ as the symbol power vector of user n and $\boldsymbol{s} = [\boldsymbol{s}_1{}', \boldsymbol{s}_2{}', \ldots, \boldsymbol{s}_K{}']'$ as the vector containing the symbol power vectors of all users. Similar vector notation will be used for other power variables, as well as for the SINR, bitrate and Lagrange dual variables. Also, define p_k^n as the line power of user n on tone k, which in the MAC is equal to s_k^n. The total line power of user n is given by

$$P^n = \sum_{k \in \mathcal{K}} p_k^n. \tag{2}$$

In a MAC, signal coordination is possible at the receiver side. Linear receiver structures are assumed, i.e. transmitted symbols are estimated from the received signal as

$$\tilde{\boldsymbol{x}}_k = \boldsymbol{R}_k^* \boldsymbol{y}_k, \tag{3}$$

where $\boldsymbol{R}_k = [\boldsymbol{r}_k^1, \boldsymbol{r}_k^2, \ldots, \boldsymbol{r}_k^N]$ is the receive matrix on tone k, containing a receive vector $\boldsymbol{r}_k^n$ for each transmitted symbol x_k^n, and where $(\cdot)^*$ denotes the Hermitian transpose operator. The signal-to-interference-plus-noise ratio (SINR) for user n on tone k is given as

$$\gamma_k^n = \frac{s_k^n |\boldsymbol{r}_k^{n*} \boldsymbol{h}_k^n|^2}{\boldsymbol{r}_k^{n*} \boldsymbol{\Sigma}_k \boldsymbol{r}_k^n + \sum_{m \in \mathcal{N} \setminus \{n\}} s_k^m |\boldsymbol{r}_k^{n*} \boldsymbol{h}_k^m|^2}, \tag{4}$$

with $\boldsymbol{\Sigma}_k$ the noise covariance matrix on tone k, $\boldsymbol{h}_k^n$ the nth column of $\boldsymbol{H}_k$, and $\cdot \setminus \cdot$ the set subtraction operator.

The optimal linear receiver in the MAC is the MMSE receiver, which maximizes the SINR of each user. Given the symbol power vector $\boldsymbol{s}_k$, the MMSE receive matrix and resulting SINR for user n are calculated as

$$\boldsymbol{R}_k = \left(\boldsymbol{H}_k \boldsymbol{S}_k \boldsymbol{H}_k{}^* + \boldsymbol{\Sigma}_k \right)^{-1} \boldsymbol{H}_k \boldsymbol{S}_k, \tag{5}$$

$$\gamma_k^n = s_k^n \boldsymbol{h}_k^{n*} (\boldsymbol{Q}_k^n)^{-1} \boldsymbol{h}_k^n, \tag{6}$$

where $\boldsymbol{S}_k = \text{diag}\{\boldsymbol{s}_k\}$, and with $\boldsymbol{Q}_k^n = \sum_{m \in \mathcal{N} \setminus \{n\}} s_k^m \boldsymbol{h}_k^m \boldsymbol{h}_k^{m*} + \boldsymbol{\Sigma}_k$ the interference-plus-noise covariance matrix of user n on tone k [25], [26]. Note that (6) provides the SINR without explicitly determining the corresponding MMSE receive matrix $\boldsymbol{R}_k$.

The linear MMSE receiver may be the optimal linear receiver, but it is not capacity achieving. The receiver structure that achieves the highest possible weighted sum rate is the non-linear MMSE-GDFE receiver [27], which sequentially decodes the signals of the different users, using the previously decoded signals to remove crosstalk from signals that are decoded subsequently. Optimizing the performance of such a receiver in practice involves finding the optimal decoding order, which is a non-trivial problem [28]. However, assuming the decoding order is fixed, the resource allocation algorithms that are presented here can be readily extended to the MMSE-GDFE case.

B. BROADCAST CHANNEL

DS transmission in an N-user DSL network can be modeled for each tone independently as

$$\boldsymbol{y}_k = \boldsymbol{H}_k{}^* \boldsymbol{T}_k \boldsymbol{x}_k + \boldsymbol{z}_k, \quad \forall k \in \mathcal{K}, \tag{7}$$

where the $N \times N$ channel matrix $[\boldsymbol{H}_k]_{n,m} = h_k^{m,n*}$ contains the complex conjugate of the transfer function between the transmitter of user n and receiver of user m, evaluated on tone k. The conjugate transpose in (7) is introduced in order to simplify notation later on.

Prior to transmission, data symbols are precoded by means of the transmit matrix $\boldsymbol{T}_k = [\boldsymbol{t}_k^1, \boldsymbol{t}_k^2, \ldots, \boldsymbol{t}_k^N]$, containing a transmit vector $\boldsymbol{t}_k^n$ for each data symbol x_k^n. The line power of line n on tone k is thus calculated as

$$p_k^n = \left[\boldsymbol{T}_k \, \text{diag}\{\boldsymbol{s}_k\} \boldsymbol{T}_k{}^* \right]_{nn}. \tag{8}$$

The SINR for user n on tone k is given as

$$\gamma_k^n = \frac{s_k^n |\boldsymbol{h}_k^{n*} \boldsymbol{t}_k^n|^2}{\sigma_k^n + \sum_{m \in \mathcal{N} \setminus \{n\}} s_k^m |\boldsymbol{h}_k^{n*} \boldsymbol{t}_k^m|^2}, \tag{9}$$

with $\boldsymbol{h}_k^n$ the n-th column of $\boldsymbol{H}_k$. The problem of finding the optimal transmit matrices $\boldsymbol{T}_k$ for the BC is more involved than selecting the optimal receive matrices $\boldsymbol{R}_k$ for the MAC, and will be addressed in Section V.

Again, linear precoding is not optimal. Higher data rates are achievable with non-linear precoders implementing dirty paper coding (DPC) [29]. A DPC-based transmitter successively encodes the symbols of the different users, such that no additional interference is caused into previously encoded users. Finding the optimal DPC transmitter in practice involves finding the optimal encoding order, which is a non-trivial problem [28]. However, once the precoding order is fixed, the resource allocation algorithms that are presented here can be readily extended to the DPC case.

C. BITLOADING AND ERROR CONTROL

When the number of users N is large, the interference-plus-noise is well approximated by a Gaussian distribution. Under this assumption, the relation between the achieved SINR, as in (3) and (9), and the achievable information bitrate b_k^n of user n on tone k is given by

$$b_k^n = b(\gamma_k^n, \rho, \Gamma) = \rho \log_2 \left(1 + \frac{\gamma_k^n}{\Gamma} \right) \tag{10}$$

with ρ the code rate and Γ the signal-to-noise ratio gap to capacity or SNR gap. Throughout this paper, the information bitrate is considered to be a continuous variable. In what follows, it is outlined how values for ρ and Γ, as well for the post-decoding byte error rate $\mathbb{P}$, are determined for a specific MC scheme.

The SNR gap Γ is determined by the target average BER, coding gain, and noise margin. In the case of zero coding gain and noise margin, assuming QAM constellations with Gray bit mapping, the SNR gap is closely approximated by

$$\Gamma_0 = -\frac{\log(5\,\text{BER})}{1.6} \tag{11}$$

with $\log(\cdot)$ the natural logarithm. For BER $\geq 10^{-3}$ and $b \geq 2$, (11) results in an overestimation of the true SNR gap by no more than 1dB [30].

Current DSL FEC mechanisms consist of a Reed-Solomon (RS) code and a trellis coded modulation (TCM) [1], [2]. The performance of the TCM is aptly modeled by including a coding gain Γ_c in the SNR gap, the value of which depends on the dimensionality of the TCM code in use [31]. Moreover, the SNR gap can include a noise margin Γ_n, which acts as a protection against non-stationary noise [32]. By including both the noise margin and the coding gain, the SNR gap becomes

$$\Gamma = \frac{\Gamma_n}{\Gamma_c}\Gamma_0. \tag{12}$$

RS codes employed in DSL networks are defined over the Galois field GF(256), implying that each RS symbol consists of one byte. A Reed-Solomon code RS(ν, κ) yields codewords of length ν, containing $\nu - \kappa$ parity symbols and κ information symbols. The RS code thus reduces the data rate of the system by a factor of $\rho_{\text{RS}} = \kappa/\nu$. The code rate is then given by

$$\rho = \rho_{\text{RS}}. \tag{13}$$

Assuming no retransmissions are possible and uncorrected errors are passed on unaltered, the post-decoding symbol (i.e. byte) error rate is given by

$$\mathbb{P} = \sum_{i=\tau+1}^{\nu} \frac{(\nu-1)!}{(\nu-i)!(i-1)!} \mathbb{P}_{\text{symb}}{}^{i}(1-\mathbb{P}_{\text{symb}})^{\nu-i}. \tag{14}$$

with $\mathbb{P}_{\text{symb}}$ the pre-decoding symbol error rate calculated as $\mathbb{P}_{\text{symb}} = 1 - (1 - \text{BER})^8$ [33], and with $\tau = \lfloor \frac{\nu-\kappa}{2} \rfloor$ the maximum number of erroneous symbols per codeword that can be corrected.

Although the approximations in this section are fairly accurate, they are only approximations and might lead to flawed DSL performance numbers. Therefore, in the simulations section, we refrain from making comments on absolute performance, and limit the discussion to mutually comparing the performance of algorithms that are developed in this paper. Moreover, it is possible to obtain more accurate estimations of the parameters ρ and Γ through extensive simulations and measurements, as in [31]. However, this paper focuses on the interaction between DSM and UEP, not on the estimation of system model parameters such as Γ and ρ.

D. UNEQUAL ERROR PROTECTION

UEP is accomplished by dividing the one connection per user into a set of subconnections, and employing a specific MC scheme for each subconnection. Each user $n \in \mathcal{N}$ has a set of subconnections $\mathcal{Q}^n$, where each subconnection $q \in \mathcal{Q}^n$ has a set of tones $\mathcal{T}_q$ associated with it. Consequently, each user decides on a tone allocation, i.e. assigns each tone $k \in \mathcal{K}$ to a single subconnection $q \in \mathcal{Q}^n$. Notice that each user transmits data over all tones $k \in \mathcal{K}$, i.e. $\mathcal{K} = \bigcup_{q\in\mathcal{Q}^n} \mathcal{T}_q$, $\forall n \in \mathcal{N}$. Furthermore, define the tone allocation of user n as $\mathcal{T}^n = \{\mathcal{T}_q | q \in \mathcal{Q}^n\}$ and the overall tone allocation as $\mathcal{T} = \{\mathcal{T}_q \mid q \in \bigcup_{n\in\mathcal{N}} \mathcal{Q}^n\}$.

Each subconnection $q \in \mathcal{Q}^n$ is offered a different level of error protection $\mathbb{P}_q$, achieved by using a specific SNR gap Γ_{0q} and resulting BER_q on each tone $k \in \mathcal{T}_q$, and by using dedicated RS and TCM codes to encode its data. Given a target $\mathbb{P}_q$ and the employed RS and TCM codes, the Γ_q required to achieve $\mathbb{P}_q$ is calculated by first inverting (14) to obtain the target pre-decoding symbol error rate $\mathbb{P}_{\text{symb}}$ and hence BER, and then applying (11) and (12).

It is often possible to achieve a single target $\mathbb{P}_q$ using various SNR gap-RS/TCM code combinations, i.e. using various MC schemes. The set of MC schemes achieving $\mathbb{P}_q$ is referred to as the MC set of subconnection q, denoted $\mathcal{M}_q$. Although achieving the same error performance, not all MC schemes in $\mathcal{M}_q$ result in the same delay and throughput performance. Therefore, care should be taken in selecting an MC scheme $i \in \mathcal{M}_q$ for each subconnection q in the DSL network.

The data rate associated with subconnection $q \in \mathcal{Q}^n$ is finally calculated as

$$R_q = f_s \sum_{k\in\mathcal{T}_q} b(\gamma_k^n, \rho_q, \Gamma_q) \tag{15}$$

with f_s the symbol rate.

III. RATE-ADAPTIVE DSM WITH UNEQUAL ERROR PROTECTION

The problem of maximizing the data rates in a DSL network by appropriately choosing symbol powers (and transmit matrices) is commonly referred to as rate-adaptive DSM [34]. Rate adaptive DSM is usually formulated as an optimization problem, where the objective is to maximize the weighted sum of the per user data rates subject to per line power constraints $P^{n,\text{tot}}$. However, here the objective is to maximize the weighted sum of the *per subconnection* data rates, i.e.

$$\begin{aligned} \max_{\substack{\boldsymbol{s},\mathcal{T} \\ \text{or} \\ \boldsymbol{s},\boldsymbol{T},\mathcal{T}}} \quad & \sum_{n\in\mathcal{N}} \sum_{q\in\mathcal{Q}^n} \omega_q R_q \\ \text{s.t.} \quad & P^n \leq P^{n,\text{tot}}, \ \forall n \in \mathcal{N} \\ & \boldsymbol{s} \in \mathbb{R}_+^{N\times K}, \end{aligned} \tag{16}$$

where the positive real weights ω_q are used to give a higher priority to some users or subconnections. In [5] and [8], the same approach towards rate-adaptive DSM with UEP has been considered for the interference channel. The decision variables of problem (16) are the symbol power vectors of all users $\boldsymbol{s}$, the overall tone allocation $\mathcal{T}$, and, whenever DS transmission is considered, the transmit matrices $\boldsymbol{T} = \left[\boldsymbol{T}_1{}', \boldsymbol{T}_2{}', \ldots, \boldsymbol{T}_K{}'\right]'$.

Note that, for now, the problem of optimally choosing an MC scheme $i \in \mathcal{M}_q$ for each $q \in \bigcup_{n\in\mathcal{N}} \mathcal{Q}^n$ is not considered in (16). In other words, problem (16) considers the case where each MC set $\mathcal{M}_q$ is a singleton. The problem of optimally choosing an MC scheme for each subconnection is addressed

in Section VI. First, the MAC and BC version of problem (16) are tackled in sections IV and V, respectively.

The tone allocation problem can be solved through primal decomposition. Observe that when the symbol power vector $\boldsymbol{s}_k$ (and the transmit matrix $\boldsymbol{T}_k$) is fixed, user n's decision to allocate tone k to a particular subconnection $q \in \mathcal{Q}^n$ does not affect the achievable value for $\omega_{\bar{q}} b_k^m(\gamma_k^m, \rho_{\bar{q}}, \Gamma_{\bar{q}})$ for any $\bar{q} \in \mathcal{Q}^m$ of user m, if $m \neq n$. In optimization terms, the tone allocation variable $\mathcal{T}$ is a "local" variable, while $\boldsymbol{s}_k$ and $\boldsymbol{T}_k$ are "complicating" variables [35]. Therefore, primal decomposition can be applied to problem (16). The per user per tone slave problem in this primal decomposition is given by

$$\ddot{b}^n(\gamma_k^n) = \max_{q \in \mathcal{Q}^n} \omega_q f_s b(\gamma_k^n, \rho_q, \Gamma_q). \tag{17}$$

The corresponding master problem is then

$$\begin{aligned} \max_{\substack{\boldsymbol{s} \\ \text{or} \\ \boldsymbol{s},\boldsymbol{T}}} \quad & \sum_{n \in \mathcal{N}} \sum_{k \in \mathcal{K}} \ddot{b}^n(\gamma_k^n) \\ \text{s.t.} \quad & P^n \leq P^{n,\text{tot}}, \ \forall n \in \mathcal{N} \\ & \boldsymbol{s} \in \mathbb{R}_+^{N \times K}. \end{aligned} \tag{18}$$

Problem (18) will be easier to solve than the original problem, as in (16). Therefore, the following sections will focus on solving (18) rather than (16).

From the definition of $\ddot{b}^n(\gamma_k^n)$, it is seen that each subconnection $q \in \mathcal{Q}^n$ has a corresponding range for γ_k^n where allocating tone k to subconnection q results in the maximum weighted information bitrate value. For subconnection $q \in \mathcal{Q}^n$, this range is more formally defined as $G_q = \left\{\gamma \in \mathbb{R}_+ \mid \ddot{b}^n(\gamma) = \omega_q f_s b(\gamma, \rho_q, \Gamma_q)\right\}$. For user n, G_q is the same on each tone k and depends solely on the values of ω_q, ρ_q, and Γ_q of each subconnection $q \in \mathcal{Q}^n$. It is readily seen that each G_q corresponds to a single closed interval. Therefore, given γ_k^n, evaluating (17) is efficiently implemented by looking up $\bar{q}$ for which $\gamma_k^n \in G_{\bar{q}}$, and subsequently calculating $\omega_{\bar{q}} f_s b(\gamma_k^n, \rho_{\bar{q}}, \Gamma_{\bar{q}})$.

Enabling all subconnections $q \in \mathcal{Q}^n$ to achieve a nonzero data rate requires G_q to be a nonempty set for each subconnection. Consider the case where user n has two subconnections $\mathcal{Q}^n = \{q_1, q_2\}$, with $\Gamma_{q_1} > \Gamma_{q_2}$. It is readily seen that $G_{q_1} = \emptyset$ if $\omega_{q_1}\rho_{q_1} < \omega_{q_2}\rho_{q_2}$. Likewise, $G_{q_2} = \emptyset$ if $\frac{\omega_{q_1}\rho_{q_1}}{\omega_{q_2}\rho_{q_2}} > \frac{\Gamma_{q_1}}{\Gamma_{q_2}}$. Care thus needs to be taken when choosing the weights ω_q. In the previous example, given ω_{q_2}, a good range of values to choose ω_{q_1} from is $\left[\omega_{q_2}\frac{\rho_{q_2}}{\rho_{q_2}}, \omega_{q_2}\frac{\Gamma_{q_1}\rho_{q_2}}{\Gamma_{q_2}\rho_{q_1}}\right]$. Another possible strategy is to let each weight depend on the instantaneous queue length of the associated subconnection.

IV. UPSTREAM DSM WITH UNEQUAL ERROR PROTECTION

In this section, two algorithms that solve the US version of the rate-adaptive DSM problem are presented: MAC-OSB-UEP achieves the global optimum of problem (18) at the cost of an exponential complexity in the number of users N; MAC-DSB-UEP exhibits lower complexity, but attains only a local optimum of problem (18). In this section, whenever problem (18) is referred to, the US version is considered.

A. GLOBALLY OPTIMAL SOLUTION: MAC-OSB-UEP

Optimization problem (18) is non-convex. Exhaustively searching for its global optimum results in an exponential complexity in NK. However, the same globally optimal solution strategy as in [8] can be employed, which is based on the optimal spectrum balancing (OSB) dual decomposition algorithm [13], [20].

The idea of dual decomposition is to solve the Lagrange dual problem associated with (18), given by

$$\min_{\boldsymbol{\lambda}} \quad g(\boldsymbol{\lambda}) \tag{19}$$

$$\text{with} \quad g(\boldsymbol{\lambda}) = \max_{\boldsymbol{s} \in \mathbb{R}_+^{N \times K}} \mathcal{L}(\boldsymbol{\lambda}, \boldsymbol{s}) \tag{20}$$

where $\boldsymbol{\lambda} = [\lambda^1, \lambda^2, \ldots, \lambda^N]'$ contains the Lagrange dual variables or Lagrange multipliers, and where the Lagrangian $\mathcal{L}(\boldsymbol{\lambda}, \boldsymbol{s})$ is defined as

$$\begin{aligned} \mathcal{L}(\boldsymbol{\lambda}, \boldsymbol{s}) &= \sum_{k \in \mathcal{K}} \mathcal{L}_k(\boldsymbol{\lambda}, \boldsymbol{s}_k) + \sum_{n \in \mathcal{N}} \lambda^n P^{n,\text{tot}} \\ \text{with} \quad \mathcal{L}_k(\boldsymbol{\lambda}, \boldsymbol{s}_k) &= \sum_{n \in \mathcal{N}} \ddot{b}^n(\gamma_k^n) - \sum_{n \in \mathcal{N}} \lambda^n p_k^n. \end{aligned} \tag{21}$$

A well known result from convex optimization states that, when some constraint qualification holds, a primal problem and its Lagrange dual problem have the same solution. Unfortunately, (18) is non-convex and the result does not apply. The primal and dual problem have different solutions, the difference being the duality gap. However, when the number of tones K is large, the time sharing property of [36] holds and the duality gap is assumed to be zero.

The Lagrange dual problem consists of a master problem (19) and a slave problem (20). Dual decomposition algorithms iteratively search for the optimal Lagrange multipliers of the master problem, solving the slave problem at every step along the way. The objective function of the master problem, i.e. the Lagrange dual function $g(\boldsymbol{\lambda})$, is convex but not differentiable. Therefore, the subgradient method [36], [37] is used to solve problem (19), which updates $\boldsymbol{\lambda}$ as

$$\lambda^{n,l+1} = \left[\lambda^{n,l} + \mu^l\left(\sum_{k=1}^{K} p_k^n - P^{n,\text{tot}}\right)\right]^+, \quad \forall n \in \mathcal{N}, \tag{22}$$

where l is the iteration number, μ^l is a scalar step size, and $[\cdot]^+ = \max(\cdot, 0)$. The subgradient method is guaranteed to converge to the optimal $\boldsymbol{\lambda}$ as long as μ^l is sufficiently small [38], and is known to exhibit a convergence rate of $\mathcal{O}(1/\sqrt{l})$. In practice however, sufficient convergence speeds can be achieved using step size scaling heuristics [38] which, assuming adequate algorithm parameters are chosen, typically result in an acceptable solution accuracy after 50-200 iterations.

From the way (21) is formulated, it is clear that the Lagrangian $\mathcal{L}(\boldsymbol{\lambda}, \boldsymbol{s})$ can be split into a sum of per tone

Algorithm 1 MAC-OSB-UEP

1: Determine G_q, $\forall q \in \bigcup_{n\in\mathcal{N}} \mathcal{Q}^n$
2: **while** distance $> \delta_P$ **do** ▷ Master Problem
3: $\mu \leftarrow 1$
4: $\boldsymbol{\lambda} \leftarrow$ best $\boldsymbol{\lambda}$ so far
5: $\Delta\boldsymbol{\lambda} \leftarrow \left(\boldsymbol{P}^{\boldsymbol{\lambda}} - \boldsymbol{P}^{\text{tot}}\right)$
6: **while** distance $\leq$ previousDistance **do**
7: previousDistance $\leftarrow$ distance
8: $\mu \leftarrow \mu \times 2$
9: $\boldsymbol{s} \leftarrow$ exhaustiveSearch$(\boldsymbol{\lambda} + \mu\Delta\boldsymbol{\lambda})$
10: $\boldsymbol{P}^{\boldsymbol{\lambda}+\mu\Delta\boldsymbol{\lambda}} \leftarrow \sum_{k\in\mathcal{K}} \boldsymbol{s}_k$
11: distance $\leftarrow \left|\boldsymbol{P}^{\text{tot}} - \boldsymbol{P}^{\boldsymbol{\lambda}+\mu\Delta\boldsymbol{\lambda}}\right|$
12: **end while**
13: **end while**
14: $\forall k \in \mathcal{K}$: calculate $\boldsymbol{R}_k$ with (5)

15: **function** exhaustiveSearch($\boldsymbol{\lambda}$) ▷ Slave Problem
16: **for** $k \in \mathcal{K}$ **do**
17: **for** $\boldsymbol{s}_k \in$ grid **do**
18: **for** $n \in \mathcal{N}$ **do**
19: Calculate γ_k^n using (6)
20: Look up $\bar{q} \in \mathcal{Q}^n$ for which $\gamma_k^n \in G_{\bar{q}}$
21: Evaluate $\omega_{\bar{q}} f_s b(\gamma_k^n, \rho_{\bar{q}}, \Gamma_{\bar{q}})$
22: **end for**
23: Calculate $\mathcal{L}_k(\boldsymbol{\lambda}, \boldsymbol{s}_k)$, retain if best so far
24: **end for**
25: **end for**
26: **end function**

Lagrangians $\mathcal{L}_k(\boldsymbol{\lambda}, \boldsymbol{s}_k)$, and a term $\sum_{n=1}^{N} \lambda^n P^{n,\text{tot}}$ which is independent of $\boldsymbol{s}$. The slave problem, consisting of maximizing $\mathcal{L}(\boldsymbol{\lambda}, \boldsymbol{s})$ as a function of the transmit spectra $\boldsymbol{s}$, can thus be solved for each tone independently through an exhaustive grid search over a discrete set of symbol power vectors $\boldsymbol{s_k}$. Given the desired solution accuracy ϵ, the number of points in the search grid is $\mathcal{O}(\epsilon^{-N})$. In other words, the resulting algorithm has a complexity that is exponential in N. The exhaustive grid search algorithm is readily seen to converge, as it is guaranteed to have found the optimum after examining each point in the search grid.

The algorithm is summarized in Algorithm 1 and is referred to as MAC-OSB with UEP (MAC-OSB-UEP). As both the subgradient algorithm and the exhaustive grid search can be proven to converge to the global optimum of the problems they solve, MAC-OSB-UEP is guaranteed to converge to the global optimum of problem (18).

The complexity difference between MAC-OSB and MAC-OSB-UEP is negligible for any reasonable value of N and $|\mathcal{Q}|$. This fact is demonstrated by the following complexity analysis of Algorithm 1. Both MAC-OSB and MAC-OSB-UEP require $I_{\text{SG}} \in [50, \ldots, 200]$ iterations for the subgradient algorithm to achieve acceptable precision, each demanding $\mathcal{O}(K\epsilon^{-N})$ evaluations of the per tone Lagrangian. The lines of Algorithm 1 involved in evaluating the per tone Lagrangian have the following asymptotic complexity. Assuming the Sherman-Morisson relation is used in the calculation of $\gamma_k^n, \forall n$ as in [23], line 19 results in $\mathcal{O}(N^3)$ complexity. Furthermore, if the intervals $G_q, \forall q \in \mathcal{Q}^n$ are stored in an interval tree, then the N queries on line 20 amount to a complexity of $\mathcal{O}(N \log|\mathcal{Q}|)$. Note that it has been assumed that $|\mathcal{Q}^n| = |\mathcal{Q}|, \forall n$. This assumption will be made in all subsequent convergence analyses. The complexity of lines 21 and 23 is respectively $\mathcal{O}(N)$ and $\mathcal{O}(1)$ per evaluation of the Lagrangian. The overall asymptotic complexity of MAC-OSB-UEP is therefore $\mathcal{O}(I_{\text{SG}} K\epsilon^{-N} N(N^2 + \log|\mathcal{Q}|))$. As MAC-OSB is obtained from MAC-OSB-UEP by deleting line 20, the complexity of MAC-OSB is $\mathcal{O}(I_{\text{SG}} K\epsilon^{-N} N^3)$. Therefore, it is concluded that Algorithm 1 adds UEP functionality to MAC-OSB without severely affecting its computational complexity.

B. LOCALLY OPTIMAL SOLUTION: MAC-DSB-UEP

Due to its exhaustive grid search with exponential complexity in N, Algorithm 1 is not practical when $N > 5$. Therefore, this subsection derives an alternative to Algorithm 1, achieving a locally optimal solution to problem (18). In each iteration of the algorithm, an approximation of (18) is constructed for each user. The sequence of solutions to these approximate problems produces a monotonically increasing objective function value, and can be shown to converge to a local optimum of (18). The algorithm derived here is a generalization of the so-called MAC-DSB algorithm for rate-adaptive spectrum management [22], and is a type of minorize-maximization (MM) algorithm.

User n's approximation of (18) is obtained by fixing the symbol power vectors $\boldsymbol{s}^m$ and tone allocation $\mathcal{T}^m$ of all users $m \neq n$, and by approximating the bitrate of users $m \neq n$ with a lower bound hyperplane. The resulting problem is not convex, yet easy to solve, and is given as

$$\begin{aligned} \max_{\boldsymbol{s}^n \in \mathbb{R}_+^K} \quad & \sum_{k\in\mathcal{K}} \ddot{b}^n(\gamma_k^n) + \sum_{k\in\mathcal{K}} a_k^n s_k^n \\ \text{s.t.} \quad & P^n \leq P^{n,\text{tot}} \\ \text{with} \quad & a_k^n = \sum_{m\in\mathcal{N}\setminus\{n\}} \omega_{q_k^m} f_s \frac{\partial b(\gamma_k^m, \rho_{q_k^m}, \Gamma_{q_k^m})}{\partial s_k^n}. \end{aligned} \tag{23}$$

In (23), $q_k^m \in \mathcal{Q}^m$ denotes the subconnection to which user m has allocated tone k. The derivatives in (23) are calculated as

$$\frac{\partial b(\gamma_k^m, \rho_{q_k^m}, \Gamma_{q_k^m})}{\partial s_k^n} = \frac{-\rho_{q_k^m}}{\log(2)} \frac{s_k^m (\boldsymbol{h}_k^{n*} (\boldsymbol{Q}_k^m)^{-1} \boldsymbol{h}_k^m)^2}{\Gamma_{q_k^m} + s_k^m \boldsymbol{h}_k^{m*} (\boldsymbol{Q}_k^m)^{-1} \boldsymbol{h}_k^m}. \tag{24}$$

Problem (23) is again solved trough dual decomposition. The Lagrange dual problem of (23) is

$$\min_{\boldsymbol{\lambda}} \quad g^n(\boldsymbol{\lambda}) \tag{25}$$

$$\text{with} \quad g^n(\boldsymbol{\lambda}) = \max_{\boldsymbol{s}^n \in \mathbb{R}_+^K} \mathcal{L}^n(\boldsymbol{s}^n, \boldsymbol{\lambda}) \tag{26}$$

where the Lagrangian is given by

$$\begin{aligned} \mathcal{L}^n(\boldsymbol{s}^n, \boldsymbol{\lambda}) &= \sum_{k\in\mathcal{K}} \mathcal{L}_k^n(s_k^n, \boldsymbol{\lambda}) + \boldsymbol{\lambda} P^{n,\text{tot}} \\ \text{with} \quad \mathcal{L}_k^n(s_k^n, \boldsymbol{\lambda}) &= \ddot{b}^n(\gamma_k^n) + s_k^n(a_k^n - \boldsymbol{\lambda}). \end{aligned} \tag{27}$$

The duality gap between (25) and (23) is assumed to be zero by virtue of the same argument as in the derivation of MAC-OSB-UEP. As the Lagrange dual function $g(\lambda)$ is convex and depends only on a single argument λ, problem (25) can be solved with a simple bisection search algorithm.

Problem (26) can again be solved for each tone independently. The per tone slave problem, defined as

$$\max_{s_k^n \geq 0} \mathcal{L}_k^n(s_k^n, \lambda), \tag{28}$$

is non-convex due to the non-smoothness of the objective function, but can be reformulated as an equivalent problem which is easier to solve.

$$\max_{q \in \mathcal{Q}^n} h(q) \tag{29}$$

$$h(q) = \max_{s_k^n \geq 0} \left[f_s \omega_q b(\gamma_k^n, \rho_q, \Gamma_q) + s_k^n \left(a_k^n - \lambda^n \right) \right] \tag{30}$$

The maximization over s_k^n will thus be executed for each $q \in \mathcal{Q}^n$, prior to selecting the subconnection q that maximizes $\mathcal{L}_k(s_k^n, \lambda)$. What remains is to solve (30). Due to the concavity of the objective function in (30), the Karush-Kuhn-Tucker (KKT) conditions provide a sufficient condition for optimality. From the system of KKT conditions, the solution to (30) is obtained as

$$s_k^n = \left[\omega_q \rho_q \frac{f_s / \log(2)}{\lambda^n - a_k^n} - \frac{\Gamma_q}{\boldsymbol{h}_k^{n*} (\boldsymbol{Q}_k^n)^{-1} \boldsymbol{h}_k^n} \right]^+. \tag{31}$$

Algorithm 2 MAC-DSB-UEP

1: **repeat**
2: **for all** $n \in \mathcal{N}$ **do**
3: $\lambda_{\min}^n \leftarrow 0$, $\lambda_{\max}^n \leftarrow \Lambda_{\max}$
4: Calculate a_k^n and $\boldsymbol{h}_k^{n*} \boldsymbol{Q}_k^{n-1} \boldsymbol{h}_k^n$, $\forall k \in \mathcal{K}$.
5: **while** $\left| \sum_k p_k^n - P^{n,\text{tot}} \right| > \delta_P$ & $\lambda^n > \delta_\lambda$ **do**
6: $\lambda^n \leftarrow \left(\lambda_{\min}^n + \lambda_{\max}^n \right) / 2$
7: **for all** k **do**
8: Calculate (s_k^n, q) as (31), $\forall q \in \mathcal{Q}^n$.
9: Select (s_k^n, q) that solves (29).
10: **end for**
11: **if** $\sum_k p_k^n > P^{n,\text{tot}}$ **then**
12: $\lambda_{\min}^n \leftarrow \lambda^n$
13: **else**
14: $\lambda_{\max}^n \leftarrow \lambda^n$
15: **end if**
16: **end while**
17: **end for**
18: **until** convergence
19: Calculate $\boldsymbol{R}_k$ using (5), $\forall k \in \mathcal{K}$

The resulting algorithm is summarized in Algorithm 2 and is referred to as MAC-DSB with UEP (MAC-DSB-UEP). Convergence of MAC-DSB-UEP is established by demonstrating that, up to a constant factor and for each value of $\boldsymbol{s}^n$, the objective function of (23) is a lower bound on the objective function of (18). Convergence then follows from the fact that the objective function of (18) is upper bounded. Note that this convergence result does not imply that Algorithm 2 converges to a stationary point of problem (18).

To see the lower bound property of the objective function of (23), first observe that each $\ddot{b}^m(\gamma_k^m)$ is a non-smooth convex function of s_k^n. This is due to $\ddot{b}^m(\gamma_k^m)$ being the pointwise supremum over a set of convex functions $\{\omega_q f_s b(\gamma_k^m, \rho_q, \Gamma_q)\}_{q \in \mathcal{Q}^n}$ of s_k^n. Therefore, a_k^n is a subderivative of $\sum_{m \in \mathcal{N} \setminus \{n\}} \ddot{b}^m(\gamma_k^m)$ as a function of s_k^n. Furthermore, $a_k^n s_k^n + c_k^n$ is an affine lower bound on $\sum_{m \in \mathcal{N} \setminus \{n\}} \ddot{b}$, where c_k^n is chosen such that $\sum_{m \in \mathcal{N} \setminus \{n\}} \ddot{b} = a_k^n s_k^n + c_k^n$ in the point of approximation. For each value of $\boldsymbol{s}^n$, the objective function of problem (23) is thus a lower bound on the objective function of problem (18), up to a constant $\sum_{k \in \mathcal{K}} c_k^n$. As each iteration of Algorithm 2 updates $\boldsymbol{s}^n$ to be the solution of problem (23), it is readily seen that each iteration of MAC-DSB-UEP increases the objective function value of both problem (23) and problem (18).

Algorithm 2 adds UEP functionality to MAC-DSB without severely affecting its computational complexity, as is demonstrated by the following asymptotic complexity analysis. Both MAC-DSB and MAC-DSB-UEP require $I_{\text{MM}} \in [10, \ldots, 50]$ iterations of the outer MM algorithm to achieve acceptable precision. For each iteration of the MM algorithm, N approximating problems are constructed (line 4) and solved (lines 5 to 16). From (24), it can be seen that line 4 requires $\boldsymbol{h}_k^{n*} \boldsymbol{Q}_k^{n-1} \boldsymbol{h}_k^n$ to be calculated for all n. As this calculation is similar to the calculation of $\gamma_k^n, \forall n$ in Algorithm 1, it has complexity $\mathcal{O}(KN^3)$ which dominates the complexity of line 4. Problem (23) is then solved by applying a bisection search algorithm to the corresponding Lagrange dual problem, which typically requires $I_{\text{BCT}} \in [2, \ldots, 20]$ iterations to achieve acceptable precision. In each iteration of the bisection search algorithm, the Lagrange dual function is evaluated by lines 8 and 9. The complexity of both lines is $\mathcal{O}(K|\mathcal{Q}|)$. Therefore, the overall asymptotic complexity of MAC-DSB-UEP is $\mathcal{O}(I_{\text{MM}} NK(N^3 + I_{\text{BCT}}|\mathcal{Q}|))$. As MAC-DSB can be obtained from MAC-DSB-UEP by deleting line 9 and executing line 8 only once for each user, it is seen that the complexity of MAC-DSB is $\mathcal{O}(I_{\text{MM}} NK(N^3 + I_{\text{BCT}}))$. It is concluded that if $N^3 + I_{\text{BCT}}$ is large compared to $I_{\text{BCT}}|\mathcal{Q}|$, Algorithm 2 adds UEP functionality to MAC-DSB without severely affecting its complexity.

V. DOWNSTREAM DSM WITH UNEQUAL ERROR PROTECTION

In this section, two algorithms that solve the DS version of the rate-adaptive DSM problem are presented: BC-OSB-UEP achieves the global optimum of problem (18) at the cost of an exponential complexity in the number of users N; BC-DSB-UEP exhibits lower complexity, but attains only a local optimum of problem (18). In this section, whenever problem (18) is referred to, the DS version is considered.

Dual decomposition again allows problem (18) to be solved for each tone independently. The Lagrange dual

problem of (18) is defined as

$$\min_{\boldsymbol{\lambda}} \quad g(\boldsymbol{\lambda}) \tag{32}$$

$$\text{with} \quad g(\boldsymbol{\lambda}) = \max_{\boldsymbol{s}\in\mathbb{R}_+^{N\times K},\boldsymbol{T}} \mathcal{L}(\boldsymbol{s},\boldsymbol{T},\boldsymbol{\lambda}) \tag{33}$$

and the Lagrangian is defined as

$$\mathcal{L}(\boldsymbol{s},\boldsymbol{T},\boldsymbol{\lambda}) = \sum_{k\in\mathcal{K}} \mathcal{L}_k(\boldsymbol{s}_k,\boldsymbol{T}_k,\boldsymbol{\lambda}) + \sum_{n\in\mathcal{N}} \lambda^n P^{n,\text{tot}}$$

$$\text{with} \quad \mathcal{L}_k(\boldsymbol{s}_k,\boldsymbol{T}_k,\boldsymbol{\lambda}) = \sum_{n\in\mathcal{N}} \left[\ddot{b}^n(\gamma_k^n) - s_k^n \boldsymbol{t}_k^{n*}\boldsymbol{\Lambda}\boldsymbol{t}_k^n\right] \tag{34}$$

where $\boldsymbol{\Lambda} = \text{diag}\{\boldsymbol{\lambda}\}$. The duality gap between the primal problem (18) and the corresponding Lagrange dual problem (32) is assumed to be zero by virtue of the same argument as in Section IV-A.

The master problem (32) is convex, not differentiable, and can again be solved with the subgradient method of Section IV-A. What remains is to solve the slave problem (33). Finding the optimal transmit matrices $\boldsymbol{T}_k$ for the BC is not as straightforward as finding the optimal receive matrices $\boldsymbol{R}_k$ for the MAC [39]. It is however possible to transform the BC slave problem into an equivalent and simpler dual MAC slave problem using MAC-BC duality theory [21], [40]–[43].

A. MAC-BC DUALITY

The MAC-BC duality theory used in this paper is based on [21], [40], and [43]. In [21] and [40], it is shown that the per tone slave problem in (33), i.e.

$$\max_{\boldsymbol{s}_k\in\mathbb{R}_+^N,\boldsymbol{T}_k} \mathcal{L}_k(\boldsymbol{s}_k,\boldsymbol{T}_k,\boldsymbol{\lambda}), \tag{35}$$

is equivalent to the per tone slave problem of a dual MAC system. The per tone Lagrangian of this dual MAC system is defined as

$$\mathcal{L}_k(\boldsymbol{\delta}_k,\boldsymbol{T}_k,\boldsymbol{\lambda}) = \sum_{n\in\mathcal{N}} \ddot{b}^n\left(\frac{\delta_k^n |\boldsymbol{t}_k^{n*}\boldsymbol{h}_k^n|^2}{\sum_{m\neq n}\delta_k^m|\boldsymbol{t}_k^{n*}\boldsymbol{h}_k^m|^2 + \boldsymbol{t}_k^{n*}\boldsymbol{\Lambda}\boldsymbol{t}_k^n}\right) - \sum_{n\in\mathcal{N}} \delta_k^n\sigma_k^n, \tag{36}$$

where δ_k^n is the symbol power of user n on tone k of the dual MAC system. The dual MAC system to which this Lagrangian function corresponds, is obtained from the original BC system in the following way: the channel matrix of the dual MAC system is the Hermitian transpose of the BC channel matrix, the dual MAC system uses the transmit vectors $\boldsymbol{t}_k^n$ from the BC system as its receive vectors, and the noise powers of the BC system $\boldsymbol{\Sigma}_k = \text{diag}\{\boldsymbol{\sigma}_k\}$ constitute the Lagrange multipliers in the dual system and vice versa.

Duality between $\mathcal{L}_k(\boldsymbol{\delta}_k,\boldsymbol{T}_k,\boldsymbol{\lambda})$ and $\mathcal{L}_k(\boldsymbol{s}_k,\boldsymbol{T}_k,\boldsymbol{\lambda})$ is established by the following two statements, which hold true for any $\boldsymbol{T}_k$:

1) For every symbol power vector $\boldsymbol{\delta}_k$, a corresponding feasible symbol power vector $\boldsymbol{s}_k$ exists such that, for each user, the achieved SINR in the BC system is the same as in the dual MAC system, and such that $\mathcal{L}_k(\boldsymbol{\delta}_k,\boldsymbol{T}_k,\boldsymbol{\lambda}) = \mathcal{L}_k(\boldsymbol{s}_k,\boldsymbol{T}_k,\boldsymbol{\lambda})$. This symbol power vector $\boldsymbol{s}_k$ can be obtained from $\boldsymbol{\delta}_k$ by solving the system of equations in (37).
2) Conversely, for every $\boldsymbol{s}_k$, it is possible to find a corresponding feasible $\boldsymbol{\delta}_k$ such that the achieved SINR is the same for each user in both systems and such that $\mathcal{L}_k(\boldsymbol{s}_k,\boldsymbol{T}_k,\boldsymbol{\lambda}) = \mathcal{L}_k(\boldsymbol{\delta}_k,\boldsymbol{T}_k,\boldsymbol{\lambda})$.

$$\boldsymbol{Z}_k\boldsymbol{s}_k = \boldsymbol{\Sigma}_k\boldsymbol{\delta}_k$$

$$[\boldsymbol{Z}_k]_{n,m} = \begin{cases} \sum_{i\neq m}\delta_k^i|\boldsymbol{t}_k^{m*}\boldsymbol{h}_k^i|^2 + \boldsymbol{t}_k^{m*}\boldsymbol{\Lambda}\boldsymbol{t}_k^m & \text{if } n=m \\ -\delta_k^n|\boldsymbol{t}_k^{m*}\boldsymbol{h}_k^n|^2 & \text{if } n\neq m \end{cases} \tag{37}$$

Both statements can be shown to be true using the same reasoning as in [43]. From this duality result, it is readily concluded that the solution of

$$\max_{\boldsymbol{\delta}_k\in\mathbb{R}_+^N,\boldsymbol{T}_k} \mathcal{L}_k(\boldsymbol{\delta}_k,\boldsymbol{T}_k,\boldsymbol{\lambda}), \tag{38}$$

when transformed to the BC domain using (37), solves the BC per tone slave problem (35).

So far it has been established that solving (38) for each tone k leads to a solution to (33) through applying the MAC-BC duality transformation from (37). As the Lagrangian in (38) corresponds to a MAC system (cf. (36)), given the symbol power vector $\boldsymbol{\delta}_k$, the optimal $\boldsymbol{T}_k$ and corresponding SINR for user n are calculated as

$$\boldsymbol{T}_k = \left(\boldsymbol{H}_k\boldsymbol{\Delta}_k\boldsymbol{H}_k{}^* + \boldsymbol{\Lambda}\right)^{-1}\boldsymbol{H}_k\boldsymbol{\Delta}_k \tag{39}$$

$$\gamma_k^n = \delta_k^n\boldsymbol{h}_k^{n*}(\boldsymbol{Q}_k^n)^{-1}\boldsymbol{h}_k^n \tag{40}$$

with $\boldsymbol{\Delta}_k = \text{diag}\{\boldsymbol{\delta}_k\}$ and $\boldsymbol{Q}_k^n = \sum_{m\in\mathcal{N}\setminus\{n\}}\delta_k^m\boldsymbol{h}_k^m\boldsymbol{h}_k^{m*} + \boldsymbol{\Lambda}$, which is similar to (5),(6). The SINR can thus again be calculated without explicitly evaluating $\boldsymbol{T}_k$. Hence, optimization over $\boldsymbol{T}_k$ can effectively be removed from (38), reducing the per tone slave problem to

$$\max_{\boldsymbol{\delta}_k\in\mathbb{R}_+^N} \mathcal{L}_k(\boldsymbol{\delta}_k,\boldsymbol{\lambda}). \tag{41}$$

B. GLOBALLY OPTIMAL SOLUTION: BC-OSB-UEP

To formulate a globally optimal algorithm for problem (18), it remains to define a procedure to solve (41). As before, an exhaustive search will be employed, for which a search grid is to be defined. This poses a specific problem. Defining boundaries for s_k^n in Section IV-A was easy, as s_k^n has a physical meaning due to its equivalence to the line power of user n on tone k. This is not the case for the virtual powers δ_k^n in the dual MAC. Therefore, it is not trivial to see what range of values for δ_k^n should be included in its search grid.

On the other hand, the SINR is a variable that does have a physical meaning in both the BC and the dual MAC. Therefore, a straightforward strategy consists of defining a search grid $\mathcal{G}$ for $\boldsymbol{\gamma}_k$, and evaluating the Lagrangian (36) for each vector $\boldsymbol{\gamma}_k \in \mathcal{G}$. Evaluating the Lagrangian for each $\boldsymbol{\gamma}_k \in \mathcal{G}$ requires finding the vector $\boldsymbol{\delta}_k$ which is mapped on to the

considered vector $\boldsymbol{\gamma}_k$ by equation (40), i.e. finding $\boldsymbol{\delta_k}$ which satisfies the following expression.

$$\boldsymbol{\delta}_k \xrightarrow{(40)} \boldsymbol{\gamma}_k \tag{42}$$

This vector $\boldsymbol{\delta}_k$ can be found using the following fixed point iteration

$$\delta_k^n(i+1) = \frac{\gamma_k^n}{\boldsymbol{h}_k^{n*}\boldsymbol{Q}_k^n(i)^{-1}\boldsymbol{h}_k^n}, \quad \forall n \in \mathcal{N} \tag{43}$$

where $\boldsymbol{Q}_k^n(i) = \sum_{m\in\mathcal{N}\setminus\{n\}} \delta_k^m(i)\boldsymbol{h}_k^m\boldsymbol{h}_k^{m*} + \boldsymbol{\Lambda}$. From [44] it is known that, independent of the starting point $\boldsymbol{\delta}_k(0)$, the fixed point iteration (43) is guaranteed to converge to the unique $\boldsymbol{\delta}_k$ that corresponds to the $\boldsymbol{\gamma}_k$. It is noted that if non-linear precoding with a predetermined encoding order is used instead of linear precoding, $\boldsymbol{\delta}_k$ can be calculated analytically from $\boldsymbol{\gamma}_k$.

The resulting algorithm is referred to as BC-OSB with UEP (BC-OSB-UEP) and is summarized in Algorithm 3. As the subgradient algorithm, the exhaustive grid search, and the fixed point iteration of (43) can all be proven to converge to the global optimum of the problems they solve, BC-OSB-UEP is guaranteed to converge to the global optimum of problem (18).

Algorithm 3 BC-OSB-UEP

1: Determine G_q, $\forall q \in \bigcup_{n\in\mathcal{N}} \mathcal{Q}^n$
2: **while** distance > tolerance **do** ▷ Master Problem
3: $\mu \leftarrow 1$
4: $\lambda \leftarrow$ best λ so far
5: $\Delta\lambda \leftarrow \left(\boldsymbol{P}^{\lambda} - \boldsymbol{P}^{\text{tot}}\right)$
6: **while** distance $\leq$ previousDistance **do**
7: previousDistance $\leftarrow$ distance
8: $\mu \leftarrow \mu \times 2$
9: $[\boldsymbol{p}, \boldsymbol{s}, \boldsymbol{T}] \leftarrow$ exhaustiveSearch$(\lambda + \mu\Delta\lambda)$
10: $\boldsymbol{P}^{\lambda+\mu\Delta\lambda} \leftarrow \sum_{k\in\mathcal{K}} \boldsymbol{p}_k$
11: distance $\leftarrow \left|\boldsymbol{P}^{\text{tot}} - \boldsymbol{P}^{\lambda+\mu\Delta\lambda}\right|$
12: **end while**
13: **end while**

14: **function** exhaustiveSearch($\boldsymbol{\lambda}$) ▷ Slave Problem
15: **for** $k \in \mathcal{K}$ **do**
16: **for** $\boldsymbol{\gamma}_k \in$ grid **do**
17: Iteratively calculate $\boldsymbol{\delta}_k$ using (43)
18: **for** $n \in \mathcal{N}$ **do**
19: Look up $\bar{q} \in \mathcal{Q}^n$ for which $\gamma_k^n \in G_{\bar{q}}$
20: Evaluate $\omega_{\bar{q}} f_s \rho_{\bar{q}} b(\gamma_k^n, \Gamma_{\bar{q}})$
21: **end for**
22: Calculate $\mathcal{L}_k(\boldsymbol{\lambda}, \boldsymbol{s}_k)$, retain if best so far
23: **end for**
24: Calculate transmit matrix $\boldsymbol{T}_k$ using (39)
25: Calculate BC user powers $\boldsymbol{s}_k$ using (37)
26: Calculate BC line powers $\boldsymbol{p}_k$ using (8)
27: **end for**
28: **end function**

The complexity analysis of Algorithm 3 is similar to that of Algorithm 1, the only major difference being that the fixed point iteration in line 17 requires $\boldsymbol{h}_k^{n*}(\boldsymbol{Q}_k^n)^{-1}\boldsymbol{h}_k^n$ to be evaluated $I_{\text{FP}} \in [1, \ldots, 5]$ times. The resulting complexity of BC-OSB-UEP is $\mathcal{O}(I_{\text{SG}} K \epsilon^{-N} N (I_{\text{FP}} N^2 + \log|\mathcal{Q}|))$. As before, BC-OSB can be obtained from BC-OSB-UEP by deleting line 19, such that the complexity of BC-OSB is $\mathcal{O}(I_{\text{SG}} K \epsilon^{-N} N^3 I_{\text{FP}})$. From this analysis, it is seen that the complexity difference between BC-OSB and BC-OSB-UEP is negligible.

C. LOCALLY OPTIMAL SOLUTION: BC-DSB-UEP

Due to its exhaustive grid search with exponential complexity in N, Algorithm 3 is not practical when $N > 5$. Therefore, this subsection derives an alternative to Algorithm 3 achieving a locally optimal solution to problem (18), which is based on an approximate evaluation of (41). Apart from this change, the resulting algorithm will be identical to Algorithm 3. In each iteration of the algorithm, an approximation of (41) is constructed for each user n. Making a similar argument as in Section IV-B, it can be shown that the sequence of solutions to these approximate problems produces a monotonically increasing objective function value that can be shown to converge to a local optimum of (41). The algorithm derived here is a generalization of the so-called BC-DSB algorithm for rate-adaptive spectrum management [23].

The approximation of (41) for user n is constructed as in Section IV-B: by fixing the symbol power δ_k^n and tone allocation q_k^m for all users $m \neq n$, and by approximating the information bitrate $b(\gamma_k^m, \rho_{q_k^m}, \Gamma_{q_k^m})$ of users $m \neq n$ with a hyperplane. The resulting problem is not convex, yet easy to solve:

$$\begin{aligned} \max_{\delta_k^n \geq 0} \quad & \ddot{b}^n(\gamma_k^n) + \delta_k^n \left(a_k^n - \sigma_k^n\right) \\ \text{with} \quad & a_k^n = \sum_{m\in\mathcal{N}\setminus\{n\}} \omega_{q_k^m} f_s \frac{\partial b(\gamma_k^m, \rho_{q_k^m}, \Gamma_{q_k^m})}{\partial \delta_k^n}, \quad \forall m,\ k \end{aligned} \tag{44}$$

where the calculation of the partial derivatives is analogous to (24). Problem (44) is akin to problem (23) in Section IV-B, and is again solved by calculating the optimal symbol power $\delta_k^{n\text{opt}}$ for every possible subconnection $q \in \mathcal{Q}^n$, and subsequently selecting the $(\delta_k^{n\text{opt}}, q)$ tuple that results in the largest value for the objective function. For fixed q, the solution to (44) can be calculated in closed form as

$$\delta_k^{n\text{opt}}(q) = \left[\frac{\omega_q \rho_q / \log(2)}{\sigma_k^n - a_k^n} - \frac{\Gamma_q}{\boldsymbol{h}_k^{n\dagger}\boldsymbol{Q}_k^{n-1}\boldsymbol{h}_k^n}\right]^+. \tag{45}$$

The resulting algorithm, referred to as BC-DSB-UEP, is identical to Algorithm 3 apart from lines 16 to 23 which are replaced by Algorithm 4. UEP functionality is added to BC-DSB by replacing the single closed form calculation of the symbol power allocation in each of the I_{MM} iterations of its inner MM algorithm with $|\mathcal{Q}^n|$ calculations of the symbol power allocation and a subconnection selection procedure. These calculations exhibit $\mathcal{O}(|\mathcal{Q}|)$ complexity. The complexity of both the BC-DSB and the BC-DSB-UEP algorithm is

Algorithm 4 Approximate Evaluation of (41) for BC-DSB-UEP

1: **while** $\boldsymbol{\delta}_k$ not converged **do**
2: **for** $n \in \mathcal{N}$ **do**
3: Calculate a_k^n
4: Calculate (δ_k^n, q) using (45), $\forall q \in \mathcal{Q}^n$
5: Select (δ_k^n, q) that maximizes objective of (44)
6: **end for**
7: **end while**

however dominated by the calculation of a_k^n (line 4) which, as was determined in Section IV-B, has complexity $\mathcal{O}(N^3)$. The complexity of BC-DSB is therefore $\mathcal{O}(I_{\text{SG}} K I_{\text{MM}} N^4)$, and that of BC-DSB-UEP is $\mathcal{O}(I_{\text{SG}} K I_{\text{MM}} N(N^3 + |\mathcal{Q}|))$. Algorithm 4 thus adds UEP functionality to BC-DSB without severely affecting its complexity.

In [36], it is pointed out that the subgradient method, which is used to update the Lagrange multipliers, is not guaranteed to converge when $g(\boldsymbol{\lambda})$ is evaluated only approximately. As the employed minorize-maximization method of Algorithm 4 cannot be guaranteed to return the global maximizer of problem (41), BC-DSB-UEP is not guaranteed to converge. However, in simulations, BC-DSB-UEP has been observed to converge in every scenario for which it has been evaluated.

VI. JOINT RESOURCE ALLOCATION AND REED-SOLOMON CODE RATE OPTIMIZATION

In Section II, it was mentioned that different modulation and coding (MC) schemes i, each characterized by a set of values (ρ_i, Γ_i), can achieve the same target $\mathbb{P}_q$. This set of MC schemes is referred to as the MC set of subconnection q, and is denoted as $\mathcal{M}_q$. As employing a large number of MC schemes in parallel adversely affects delay performance, only a single MC scheme $i \in \mathcal{M}_q$ should be used per subconnection q.

Different MC schemes result in different performance. Consider two schemes $i_1, i_2 \in \mathcal{M}_q$ with the same value for ν_i and achieving the same $\mathbb{P}_q$, but for which $\Gamma_{i_1} < \Gamma_{i_2}$ and $\kappa_{i_1} < \kappa_{i_2}$. As $\rho_{i_1} < \rho_{i_2}$, MC scheme i_1 incurs a larger multiplicative bitrate overhead than i_2. However, i_2 employs a larger SNR gap, resulting in an approximately additive overhead as compared to i_1. Therefore, it is more appealing to use i_2 when γ_k^n is high on all tones $k \in \mathcal{T}_q$ and vice versa. It is seen that the optimal choice for $i \in \mathcal{M}_q$ depends on the value for the achieved SINR on all tones $k \in \mathcal{T}_q$. The MC scheme selection should therefore be optimized conjointly with $\boldsymbol{s}$, $\boldsymbol{T}$, and $\mathcal{T}$.

In general, jointly selecting an optimal resource allocation and MC scheme is referred to as adaptive modulation and coding (AMC). In the context of DSL networks incorporating UEP, AMC can be formulated as the following optimization problem:

$$\begin{aligned} \max_{\substack{\boldsymbol{s},\mathcal{T},\boldsymbol{i}\in\mathcal{M} \\ \text{or} \\ \boldsymbol{s},\boldsymbol{T},\mathcal{T},\boldsymbol{i}\in\mathcal{M}}} \quad & \sum_{n\in\mathcal{N}} \sum_{q\in\mathcal{Q}^n} \omega_q R_q \\ \text{s.t.} \quad & P^n \leq P^{n,\text{tot}}, \ \forall n \in \mathcal{N} \\ & \boldsymbol{s} \in \mathbb{R}_+^{N\times K}, \end{aligned} \tag{46}$$

with $\mathcal{M} = \prod_{n\in\mathcal{N}} \prod_{q\in\mathcal{Q}^n} \mathcal{M}_q$, and where $\boldsymbol{i}$ is a vector containing an element i_q for each $q \in \bigcup_{n\in\mathcal{N}} \mathcal{Q}^n$ signifying the MC scheme employed by subconnection q. The optimal choice for i_q depends on the achieved SINR on all tones $k \in \mathcal{T}_q$. Consequently, problem (46) is coupled over all tones by both the total power constraints and the MC scheme selection problem. This coupling makes problem (46) hard to solve directly.

The proposed strategy is to formulate a relaxation of problem (46), the solution of which is then used to select an MC scheme for each subconnection. In addition, the solution to the relaxed problem yields an upper bound on throughput performance. After having selected an MC scheme for each subconnection, problem (46) reduces to problem (16), which is solved to obtain the final resource allocation.

Consider the relaxation of problem (46) obtained by abandoning the constraint that a single MC scheme is used for each subconnection. Instead, let each MC scheme $i \in \mathcal{M}_q$ for each subconnection q itself constitute a distinct subconnection with which a set of tones $\mathcal{T}_i$ is associated. In addition, define $\tilde{\mathcal{T}} = \{\mathcal{T}_i \mid i \in \bigcup_{n\in\mathcal{N}} \bigcup_{q\in\mathcal{Q}^n} \mathcal{M}_q\}$. The obtained relaxed problem will be referred to as the multiple MC relaxation (MMCR) of problem (46), and is formulated as

$$\begin{aligned} \max_{\substack{\boldsymbol{s},\tilde{\mathcal{T}} \\ \text{or} \\ \boldsymbol{s},\boldsymbol{T},\tilde{\mathcal{T}}}} \quad & \sum_{n\in\mathcal{N}} \sum_{q\in\mathcal{Q}^n} \omega_q \sum_{i\in\mathcal{M}_q} R_i \\ \text{s.t.} \quad & P^n \leq P^{n,\text{tot}}, \ \forall n \in \mathcal{N} \\ & \boldsymbol{s} \in \mathbb{R}_+^{N\times K}, \end{aligned} \tag{47}$$

where, as before, R_i denotes the data rate achieved by subconnection i of user n. Moreover, a system which simultaneously employs multiple MC schemes to achieve a single target $\mathbb{P}_q$ is referred to as a multiple MC (MMC) system, as opposed to a one MC (OMC) system employing only a single MC scheme for each target $\mathbb{P}_q$. From an optimization point of view, problem (47) is fully equivalent to problem (16). Consequently, the algorithms developed in Sections IV and V can be applied to obtain a solution $(\boldsymbol{s}, \tilde{\mathcal{T}})^{\text{MMCR}}$ or $(\boldsymbol{s}, \boldsymbol{T}, \tilde{\mathcal{T}})^{\text{MMCR}}$.

This solution is then used to heuristically decide which MC scheme is to be employed for each subconnection $q \in \bigcup_{n\in\mathcal{N}} \mathcal{Q}^n$ as follows. The MC scheme for subconnection q is selected as $i \in \mathcal{M}_q$ maximizing the data rate of subconnection q, i.e.

$$i_q = \arg\max_{i\in\mathcal{M}_q} R_q, \tag{48}$$

where it is assumed that q employs tones $\mathcal{T}_q = \bigcup_{i\in\mathcal{M}_q} \mathcal{T}_i^{\text{MMCR}}$, and where the resource allocation $\boldsymbol{s}^{\text{MMCR}}$ or $(\boldsymbol{s}, \boldsymbol{T})^{\text{MMCR}}$ is used in calculating R_q. The resulting algorithm is referred to as the MMCR-based rate selection (MMCR-RS) algorithm. After having selected an MC scheme for each subconnection, problem (46) reduces to problem (16), which is solved to obtain the final resource allocation.

The MMC system provides an upper bound on the performance of the corresponding OMC system.

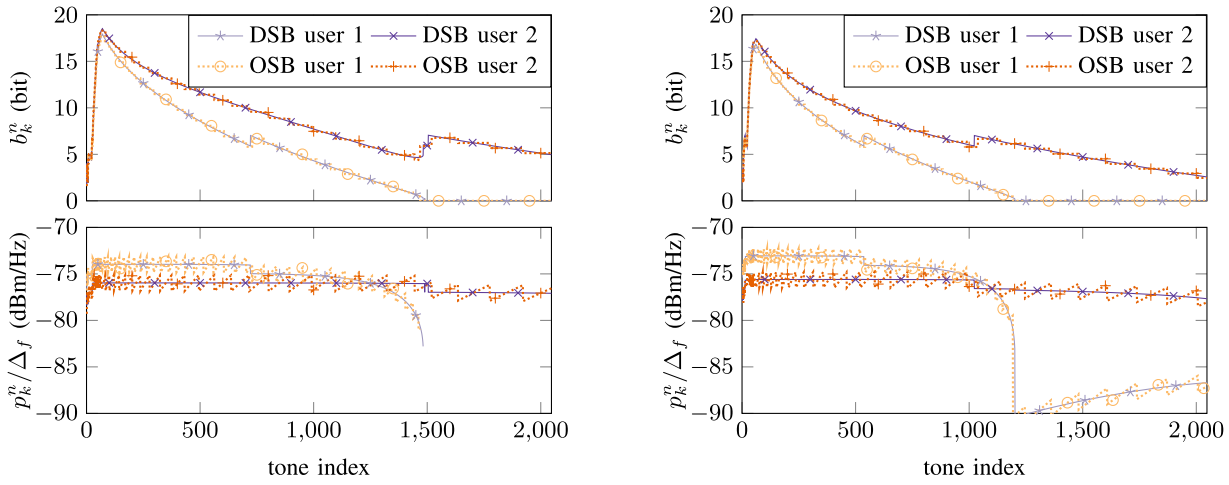

FIGURE 1. Information bitrate and transmit spectrum for two user US (left) and DS (right) G.fast systems. In the legend, OSB and DSB have been used as an abbreviation of MAC-OSB-UEP and BC-OSB-UEP, and of MAC-DSB-UEP and BC-DSB-UEP, respectively.

TABLE 1. Data rates for two user US and DS systems, in MBit/s.

	MAC-OSB-UEP		MAC-DSB-UEP		BC-OSB-UEP		BC-DSB-UEP	
	user 1	user 2	user 1	user 2	user 1	user 2	user 1	user 2
q_1	363.1	706.8	361.2	702.1	260.8	490.1	259.4	486.3
q_2	130.8	155.7	134.1	161.3	112.2	231.0	109.3	224.4
WRS	1299.1		1299.6		1025.5		1012.7	

More specifically, consider the aggregate data rate of all subconnections achieving $\mathbb{P}_q$ in an MMC system, calculated as $R_q^{\text{MMCR}} = \sum_{i \in \mathcal{M}_q} R_i$. For each feasible point of problem (46) with corresponding data rates $\check{R}_q$, there exists a feasible point of problem (47) with corresponding aggregate data rates $\hat{R}_q^{\text{MMCR}}$, for which $\check{R}_q \leq \hat{R}_q^{\text{MMCR}}$, $\forall q \in \mathcal{Q}^n$, $\forall n \in \mathcal{N}$. Therefore, the set of achievable rates in the MMC system is a superset of the set of achievable rates in the corresponding OMC system. In the simulations, this upper bound property is used to assess the performance of the MMCR-RS algorithm.

VII. SIMULATION RESULTS

In this section, simulation results are shown for the algorithms presented in Sections IV, V and VI. Differences in performance between the OSB and DSB algorithms are assessed in Section VII-A. The performance of the MMCR-RS algorithm is assessed in Section VII-B.

Parameter settings for all experiments are as follows. It is assumed that the twisted pair line diameter is 0.5 mm, which corresponds to 24AWG. For G.fast, the tone spacing is $\Delta_f = 51.750\,\text{kHz}$, the symbol rate is $f_s = 48\,\text{kHz}$, the maximum line power is $P^{\text{tot}} = 4\,\text{dBm}$, and the number of tones is $K = 2047$ [2]. The values for the coding gain and noise margin are respectively set to $\Gamma_c = 3\,\text{dB}$, resulting from a 2D TCM [31], and $\Gamma_n = 6\,\text{dB}$.

A. PERFORMANCE COMPARISON BETWEEN OSB AND DSB ALGORITHMS

The differences between the OSB and DSB algorithms are analyzed in a network containing 2 users. The twisted pair line lengths are chosen to be 200m and 110m for user 1 and user 2, respectively. Each user supports two subconnections q_1 and q_2, achieving error rates $\text{BER}_{q_1} = 10^{-7}$ and $\text{BER}_{q_2} = 10^{-3}$. RS coding is applied to neither of the subconnections. The error rates, combined Γ_n and Γ_c, result in SNR gaps $\Gamma_{q_1} = 12.6\,\text{dB}$ and $\Gamma_{q_2} = 8.2\,\text{dB}$. For each user n, the weights are chosen as $\omega_{q_1} = 1$ and $\omega_{q_2} = 0.8$.

The information bitrate and power loading resulting from MAC-OSB-UEP and MAC-DSB-UEP, as well as from BC-OSB-UEP and BC-DSB-UEP, are shown in FIGURE 1. The data rate achieved for each individual subconnection is given in TABLE 1. Both TABLE 1 and FIGURE 1 demonstrate that the solutions found by the DSB algorithms are very similar to the solutions found by the OSB algorithms. In the US channel, MAC-OSB-UEP performs even slightly worse than MAC-DSB-UEP. This is explained by the discrete grid search of MAC-OSB-UEP, which, due to its finite granularity, can result in a slightly suboptimal solution when compared to MAC-DSB-UEP.

In the power loading curves of FIGURE 1 it is seen that, even though user 1 is not using any tones above $k = 1202$, its line power p_k^1 is nonzero. It is noted that, due to the precoding operation using transmit matrix $\boldsymbol{T}_k$, each line power p_k^n depends on the symbol powers s_k^m of all users m. The nonzero line power of user 1 thus results from user 1 encoding its symbols with a transmit vector $\boldsymbol{t}_k^2$ containing two nonzero entries. Due to increased crosstalk at high frequencies, linear precoding increases line powers, making it highly suboptimal. As stated in [23], this suboptimality can be alleviated using non-linear precoding techniques.

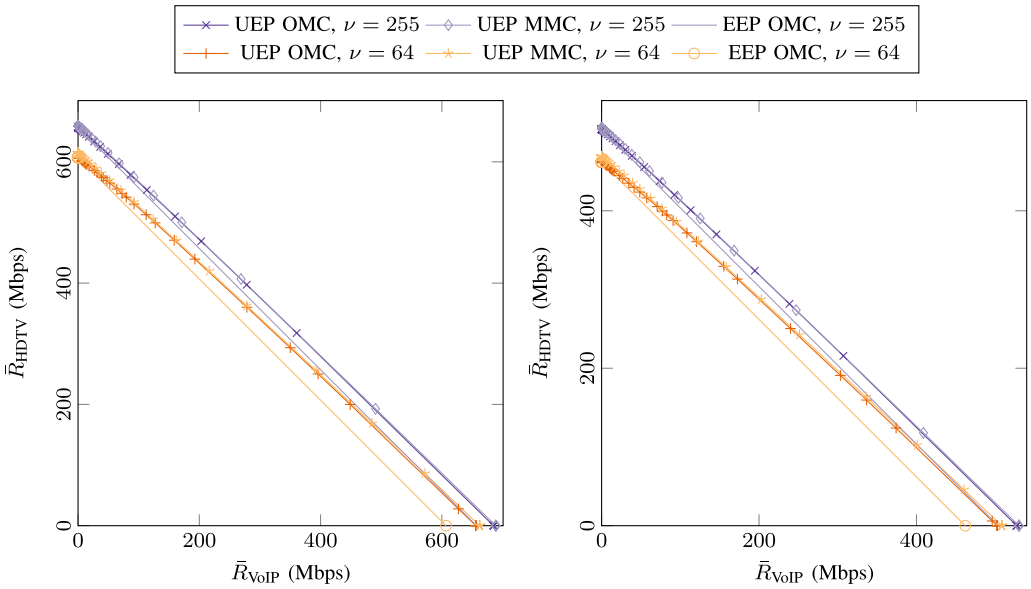

FIGURE 2. Achievable rate region of 10 user US (left) and DS (right) G.fast systems using RS codewords either of length $\nu = 64$, or of length $\nu = 255$. For each scenario, three rate region are drawn: one for an OMC UEP system, one for the corresponding MMC UEP system, and one for an OMC EEP system servicing a single subconnection achieving $\mathbb{P}_{\text{HDTV}}$.

Some discontinuities can be observed in the curves in FIGURE 1, originating from a change in tone allocation. For example, the bitrate curve of user 2 in the DS system is discontinuous at tone $k = 13$, where the tone allocation changes from q_2 to q_1, and at tone $k = 1022$, where the tone allocation changes back to q_2. Differences between tones belonging to q_1 and q_2 show how UEP improves performance. Obviously, lower error protection results in an increased information bitrate. Furthermore, less power is consumed on tones with lower error protection reducing crosstalk and, in addition, providing the opportunity to use the retained power elsewhere.

B. MMCR-RS PERFORMANCE ANALYSIS

The performance of the MMCR-RS algorithm is analyzed for a larger DSL network. The network under consideration connects 10 users to a distribution point. The distance between users and distribution point ranges from 200m for user 1 down to 110m for user 10, decreasing with 10m for each consecutive user. DSB algorithms are employed to calculate the resource allocation.

Target byte error rates $\mathbb{P}_q$ are chosen to be representative for VoIP and HDTV applications. For VoIP, it is assumed that the G.711 audio codec is used with payload size of 240 codec bytes per IP packet, resulting in an overall average IP packet size of 381 bytes [45]. Combined with an acceptable packet loss rate of 1% [46], the allowable physical layer byte error rate is $2.62 \cdot 10^{-5}$, which is rounded down to $\mathbb{P}_{\text{VoIP}} = 10^{-5}$ in simulations. Likewise, the IP average packet size for MPEG-2 based HDTV is 1316 byte, and the acceptable packet loss rate is 10^{-6} [47]. This results in the requirement that $\mathbb{P}_{\text{HDTV}} \leq 7.6 \cdot 10^{-10}$, simplified to $\mathbb{P}_{\text{HDTV}} = 10^{-10}$ in simulations. The above calculations assume that each uncorrected error results in an IP packet loss.

Fixed RS codeword lengths of either $\nu = 64$ or $\nu = 255$ are employed [2]. The MC sets $\mathcal{M}_q$ of all subconnections contain an element i for each allowable number of parity symbols per RS codeword, specified in [2] as $\nu - \kappa_i = 0, 2, \ldots, 16$, such that $|\mathcal{M}_q| = 9$, $\forall q \in \mathcal{Q}^n, \forall n \in \mathcal{N}$. The value of each Γ_i can then be calculated from ν, κ_i and $\mathbb{P}_q$, as explained in Section II-D.

Results for the MMCR-RS algorithm are visualized by drawing the rate region of different DSL networks, containing all achievable combinations $(\bar{R}_{\text{VoIP}}, \bar{R}_{\text{HDTV}})$ of the average data rates $\bar{R}_q = \frac{1}{N} \sum_{n \in \mathcal{N}} R_q$, which assumes that $q \in \mathcal{Q}^n$, $\forall n \in \mathcal{N}$. Edge points of this rate region can be calculated by maximizing $\omega_{\text{VoIP}} \bar{R}_{\text{VoIP}} + \omega_{\text{HDTV}} \bar{R}_{\text{HDTV}}$ for different values for the weights ω_q [13]. Values for ω_{VoIP} range from 0.4 to 0.5, and ω_{HDTV} is set to $1 - \omega_{\text{VoIP}}$.

FIGURE 2 displays the edges of three rate regions for a set of four different DSL networks. The rate regions labeled 'UEP OMC' correspond to OMC systems employing the MMCR-RS algorithm to select an MC scheme for each subconnection, and subsequently using either MAC-DSB-UEP or BC-DSB-UEP to solve (16). The rate regions labeled 'UEP MMC' correspond to MMC systems employing either MAC-DSB-UEP or BC-DSB-UEP to solve (47), and for which R_q is calculated as the aggregate data rate of all subconnections achieving $\mathbb{P}_q$. As the UEP MMC rate region is a superset of the UEP OMC rate region, the UEP MMC rate region is an upper bound for the UEP OMC rate region. The rate regions of the OMC systems employing MMCR-RS mostly coincide with their respective MMC upper bounds,

indicating that the MMCR-RS algorithm performs very well. Moreover, this result demonstrates that using a single MC scheme per subconnection has little impact on the performance of the DSL network.

The rate regions labeled 'EEP OMC' correspond to equal error protection (EEP) DSL networks achieving $\mathbb{P}_{\text{HDTV}}$ for both applications. The achievable data rates of the UEP DSL networks are clearly higher than those of the EEP DSL networks, indicating the benefit of employing UEP in DSL. It is noted that for $\nu = 255$, the gain of UEP over EEP is rather small. However, the considered EEP systems do employ MMCR-RS to decide which MC scheme to employ for each user. In other words, the developed UEP algorithms helped attaining the optimal EEP DSL performance. Therefore, even though the UEP *architecture* may lack advantages in some scenarios, the proposed UEP *algorithms* do not.

VIII. CONCLUSION

Four new DSM algorithms have been presented for joint signal and spectrum coordination in DSL networks providing UEP. Two OSB algorithms are provided: one for upstream and one for downstream DSL networks, both exhibiting exponential complexity in the number of users. In addition, two DSB algorithms are provided that only converge to a local optimum. However, simulations have shown that the solutions found by the DSB algorithms largely coincide with solutions found by the corresponding OSB algorithms, at only a fraction of the computation time. In addition, the MMCR-RS algorithm for MC scheme selection has been developed. Simulations have shown that MMCR-RS algorithm performs very well, and that using a single MC scheme per subconnection does not have a large impact on the performance of the DSL network. Results have also shown the benefit of UEP, as compared to EEP, as it is able to achieve moderate performance gains.

REFERENCES

[1] *Very High Speed Digital Subscriber Line Transceivers 2 (VDSL2)*, document ITU-T G.993.2, 2015.

[2] *Fast Access to Subscriber Terminals (G.Fast)—Physical Layer Specification*, document ITU-T G.9701, 2014.

[3] Y. Huo, C. Hellge, T. Wiegand, and L. Hanzo, "A tutorial and review on inter-layer FEC coded layered video streaming," *IEEE Commun. Surveys Tuts.*, vol. 17, no. 2, pp. 1166–1207, 2nd Quart., 2015.

[4] W. Henkel, K. Hassan, N. von Deetzen, S. Sandberg, L. Sassatelli, and D. Declercq, "UEP concepts in modulation and coding," *Adv. Multimedia*, vol. 2010, Jun. 2010, Art. no. 416797. [Online]. Available: https://www.hindawi.com/journals/am/2010/416797/

[5] A. McKinley and A. Marshall, "An optimal multi-user, multi-service algorithm for dynamic spectrum management in DSL," in *Proc. IEEE Int. Conf. Telecommun.*, Jun. 2008, pp. 1–5.

[6] T. Brüggen and P. Vary, "Unequal error protection by modulation with unequal power allocation," *IEEE Commun. Lett.*, vol. 9, no. 6, pp. 484–486, Jun. 2005.

[7] H. Zheng and K. J. R. Liu, "Power minimization for delivering integrated multimedia services over digital subscriber line," *IEEE J. Sel. Areas Commun.*, vol. 18, no. 6, pp. 841–849, Jun. 2000.

[8] J. Verdyck, P. Tsiaflakis, and M. Moonen, "Unequal error protection in rate adaptive spectrum management for digital subscriber line systems," in *Proc. 23rd Eur. Signal Process. Conf. (EUSIPCO)*, Nice, France, Aug./Sep. 2015, pp. 1451–1455.

[9] J. M. Cioffi, S. Jagannathan, and W. Lee, "Digital subscriber line (DSL)," *Scholarpedia*, vol. 3, no. 8, p. 3995, Aug. 2008.

[10] ATIS SYNC committee. (Nov. 2012). *Dynamic Spectrum Management Technical Report, Issue 2*, ATIS, Washington, DC, USA. [Online]. Available: https://www.atis.org/docstore/product.aspx?id=27861

[11] W. Yu, G. Ginis, and J. M. Cioffi, "Distributed multiuser power control for digital subscriber lines," *IEEE J. Sel. Areas Commun.*, vol. 20, no. 5, pp. 1105–1115, Jun. 2002.

[12] J. M. Cioffi, W. Rhee, M. Mohseni, and M. H. Brady, "Band preference in dynamic spectrum management," in *Proc. 12th Eur. Signal Process. Conf.*, Vienna, Austria, Sep. 2004, pp. 1205–1208.

[13] R. Cendrillon, W. Yu, M. Moonen, J. Verlinden, and T. Bostoen, "Optimal multiuser spectrum balancing for digital subscriber lines," *IEEE Trans. Commun.*, vol. 54, no. 5, pp. 922–933, May 2006.

[14] D. Statovci, T. Nordström, and R. Nilsson, "The normalized-rate iterative algorithm: A practical dynamic spectrum management method for DSL," *EURASIP J. Adv. Signal Process.*, vol. 2006, p. 095175, Dec. 2006. [Online]. Available: https://link.springer.com/article/10.1155/ASP/2006/95175

[15] J. Papandriopoulos and J. S. Evans, "SCALE: A low-complexity distributed protocol for spectrum balancing in multiuser DSL networks," *IEEE Trans. Inf. Theory*, vol. 55, no. 8, pp. 3711–3724, Aug. 2009.

[16] P. Tsiaflakis and M. Moonen, "Low-complexity dynamic spectrum management algorithms for digital subscriber lines," in *Proc. IEEE Int. Conf. Acoust., Speech Signal Process.*, Mar./Apr. 2008, pp. 2769–2772.

[17] G. Ginis and J. M. Cioffi, "Vectored transmission for digital subscriber line systems," *IEEE J. Sel. Areas Commun.*, vol. 20, no. 5, pp. 1085–1104, Jun. 2002.

[18] R. Cendrillon, G. Ginis, E. V. D. Bogaert, and M. Moonen, "A near-optimal linear crosstalk canceler for upstream VDSL," *IEEE Trans. Signal Process.*, vol. 54, no. 8, pp. 3136–3146, Aug. 2006.

[19] R. Cendrillon, G. Ginis, E. V. D. Bogaert, and M. Moonen, "A near-optimal linear crosstalk precoder for downstream VDSL," *IEEE Trans. Commun.*, vol. 55, no. 5, pp. 860–863, May 2007.

[20] P. Tsiaflakis, J. Vangorp, J. Verlinden, and M. Moonen, "Multiple access channel optimal spectrum balancing for upstream DSL transmission," *IEEE Commun. Lett.*, vol. 11, no. 4, pp. 300–398, Apr. 2007.

[21] V. L. Nir, M. Moonen, J. Verlinden, and M. Guenach, "Optimal power allocation for downstream xDSL with per-modem total power constraints: Broadcast channel optimal spectrum balancing (BC-OSB)," *IEEE Trans. Signal Process.*, vol. 57, no. 2, pp. 690–697, Feb. 2009.

[22] P. Tsiaflakis, R. B. Moraes, and M. Moonen, "A low-complexity algorithm for joint spectrum and signal coordination in upstream DSL transmission," in *Proc. 18th IEEE Symp. Commun. Veh. Technol. Benelux (SCVT)*, Nov. 2011, pp. 1–6.

[23] W. Lanneer, M. Moonen, P. Tsiaflakis, and J. Maes, "Linear and nonlinear precoding based dynamic spectrum management for downstream vectored G.fast transmission," in *Proc. IEEE Global Commun. Conf. (GLOBECOM)*. San Diego, CA, USA, Dec. 2015, pp. 1–6.

[24] R. B. Moraes, P. Tsiaflakis, J. Maes, and M. Moonen, "DMT MIMO IC rate maximization in DSL with combined signal and spectrum coordination," *IEEE Trans. Signal Process.*, vol. 61, no. 7, pp. 1756–1769, Apr. 2013.

[25] U. Madhow and M. L. Honig, "MMSE interference suppression for direct-sequence spread-spectrum CDMA," *IEEE Trans. Commun.*, vol. 42, no. 12, pp. 3178–3188, Dec. 1994.

[26] N. Kim, Y. Lee, and H. Park, "Performance analysis of MIMO system with linear MMSE receiver," *IEEE Trans. Wireless Commun.*, vol. 7, no. 11, pp. 4474–4478, Nov. 2008.

[27] J. M. Cioffi and G. D. Forney, Jr., "Generalized decision-feedback equalization for packet transmission with ISI and Gaussian noise," in *Communications, Computation, Control, and Signal Processing*, A. Paulraj, V. Roychowdhury, and C. D. Schaper, Eds. Boston, MA, USA: Springer, 1997, pp. 79–127.

[28] A. R. Forouzan, M. Moonen, J. Maes, and M. Guenach, "Efficient calculation of the MMSE-GDFE decoding order in non-ideal DSL multiple-access channels," in *Proc. 17th IEEE Symp. Commun. Veh. Technol. Benelux (SCVT)*, Nov. 2010, pp. 1–6.

[29] M. H. M. Costa, "Writing on dirty paper (Corresp.)," *IEEE Trans. Inf. Theory*, vol. 29, no. 5, pp. 439–441, May 1983.

[30] S. T. Chung and A. J. Goldsmith, "Degrees of freedom in adaptive modulation: A unified view," *IEEE Trans. Commun.*, vol. 49, no. 9, pp. 1561–1571, Sep. 2001.

[31] J. Neckebroek, "Error correction, precoding and bitloading algorithms in high-speed access networks," Ph.D. dissertation, Ghent Univ., Gent, Belgium, 2016.
[32] E. V. den Bogaert, T. Bostoen, J. Verlinden, R. Cendrillon, and M. Moonen, "ADSL transceivers applying DSM and their nonstationary noise robustness," *EURASIP J. Adv. Signal Process.*, vol. 2006, no. 1, p. 067686, Dec. 2006. [Online]. Available: https://link.springer.com/article/10.1155/ASP/2006/67686
[33] S. B. Wicker, *Reed-Solomon Codes and Their Applications*. Piscataway, NJ, USA: IEEE Press, 1994.
[34] T. Starr, J. M. Cioffi, and P. Silverman, *Understanding Digital Subscriber Line Technology*. Englewood Cliffs, NJ, USA: Prentice-Hall, 1999.
[35] S. Boyd, L. Xiao, A. Mutapcic, and J. Mattingley, "Notes on decomposition methods," Stanford Univ., Stanford, CA, USA, Appl. Note EE364B, 2007, pp. 1–36.
[36] W. Yu and R. Lui, "Dual methods for nonconvex spectrum optimization of multicarrier systems," *IEEE Trans. Commun.*, vol. 54, no. 7, pp. 1310–1322, Jul. 2006.
[37] D. P. Bertsekas, *Nonlinear Programming*, 2nd ed. Belmont, MA, USA: Athena Scientific, Sep. 1999.
[38] P. Tsiaflakis, J. Vangorp, M. Moonen, and J. Verlinden, "A low complexity optimal spectrum balancing algorithm for digital subscriber lines," *Signal Process.*, vol. 87, no. 7, pp. 1735–1753, Jul. 2007.
[39] M. Schubert and H. Boche, "Joint 'dirty paper' pre-coding and downlink beamforming," in *Proc. IEEE 7th Int. Symp. Spread Spectr. Techn. Appl.*, vol. 2. Sep. 2002, pp. 536–540.
[40] W. Yu and T. Lan, "Transmitter optimization for the multi-antenna downlink with per-antenna power constraints," *IEEE Trans. Signal Process.*, vol. 55, no. 6, pp. 2646–2660, Jun. 2007.
[41] F. Rashid-Farrokhi, K. J. R. Liu, and L. Tassiulas, "Transmit beamforming and power control for cellular wireless systems," *IEEE J. Sel. Areas Commun.*, vol. 16, no. 8, pp. 1437–1450, Oct. 1998.
[42] E. Visotsky and U. Madhow, "Optimum beamforming using transmit antenna arrays," in *Proc. IEEE 49th Veh. Technol. Conf.*, vol. 1. Jul. 1999, pp. 851–856.
[43] R. Hunger, M. Joham, and W. Utschick, "On the MSE-duality of the broadcast channel and the multiple access channel," *IEEE Trans. Signal Process.*, vol. 57, no. 2, pp. 698–713, Feb. 2009.
[44] M. Schubert and H. Boche, "A generic approach to QoS-based transceiver optimization," *IEEE Trans. Commun.*, vol. 55, no. 8, p. 1557–1566, Aug. 2007.
[45] Cisco Systems. *Voice Codec Calculator*. Accessed: Sep. 2, 2017. [Online]. Available: https://cway.cisco.com/tools/vccalc/
[46] *End-User Multimedia QoS Categories*, Standard ITU-T G.1010, 2001.
[47] "Triple-play services quality of experience (QoE) requirements," DSL-Forum, Arch. Transp. Work. Group, Fremont, CA, USA, Tech. Rep. TR-126, 2006.



JEROEN VERDYCK (S'15) received the M.Sc. degree in electrical engineering from KU Leuven, Leuven, Belgium, in 2014, where he is currently pursuing the Ph.D. degree with the Electrical Engineering Department, under the supervision of Prof. M. Moonen. He is involved in joint projects with KU Leuven and the University of Antwerp, Antwerp, Belgium. His research interests include signal processing and optimization for digital communication systems with an emphasis on DSL wireline access networks.



MARC MOONEN (M'94–SM'06–F'07) is currently a Full Professor with the Electrical Engineering Department, KU Leuven, where he is also the Head of the research team involved in the area of numerical algorithms and signal processing for digital communications, wireless communications, DSL, and audio signal processing.

Dr. Moonen was the Chairman of the IEEE Benelux Signal Processing Chapter from 1998 to 2002, a member of the IEEE Signal Processing Society Technical Committee on Signal Processing for Communications, and the President of EURASIP (2007–2008 and 2011–2012). He is currently a member of the Editorial Board of the *EURASIP Journal on Advances in Signal Processing*.

He was a recipient of the 1994 KU Leuven Research Council Award, the 1997 Alcatel Bell (Belgium) Award (with P. Vandaele), and the 2004 Alcatel Bell (Belgium) Award (with R. Cendrillon). He was a 1997 Laureate of the Belgium Royal Academy of Science. He received best paper awards from the IEEE TRANSACTIONS ON SIGNAL PROCESSING (with G. Leus and D. Giacobello) and the *Signal Processing* (with S. Doclo).

He has served as an Editor-in-Chief of the *EURASIP Journal on Applied Signal Processing* from 2003 to 2005 and an Area Editor for feature articles in the *IEEE Signal Processing Magazine* from 2012 to 2014. He has been a member of the Editorial Board of the IEEE TRANSACTIONS ON CIRCUITS AND SYSTEMS II, the *IEEE Signal Processing Magazine*, the *Integration*, the VLSI journal, the *EURASIP Journal on Wireless Communications and Networking*, and the *Signal Processing*.